Study of the nuclear spatial structure of neutron-rich B and C isotopes by proton elastic scattering in inverse kinematics

G.D. Alkhazov[1)], A. Bleile[2)], A.V. Dobrovolsky[1)], P. Egelhof[2)], H. Geissel[2)], S. Ilieva[2)], A.G. Inglessi[1)], A.V. Khanzadeev[1)], O.A. Kisselev[1,2)], G.A. Korolev[1)], Yu. Litvinov[2)], M. Mutterer[2)], C. Scheidenberger[2)], D.M. Seliverstov[1)], A.A. Vorobyov[1)], H. Weik[2)], V.I. Yatsoura[1)], A.A. Zhdanov[1)]

1) Petersburg Nuclear Physics Institute, Gatchina, Russia
2) Gesellschaft fur Schwerionenforschung, Dar.m.s.tadt

Abstract: We propose to study nuclear sizes and shapes of isotopic chains ^{11}B, ^{13}B, ^{14}B, ^{15}B and ^{12}C, ^{14}C, ^{15}C, ^{16}C, ^{17}C by small-angle proton elastic scattering in inverse kinematics. The nuclear density distributions will be established from the measured differential cross sections by applying the Glauber multiple scattering theory. The accurate determination of the size and radial shape of the nuclear matter distribution allows one to study the development of halo like structures in the neutron-rich nuclei.

To study the evolution of nuclear sizes and shapes of nuclei from the valley of beta-stability to the drip-line is one of the central tasks of modern nuclear structure physics. Recent techniques with radioactive beams have made it possible to reach the limit of the neutron drip line for relatively light nuclei. Experimental studies have lead to a discovery of significant neutron halos (skins) in these neutron-rich exotic nuclei, such as ^{6}He, ^{8}He, ^{11}Li and ^{11}Be. In nuclei near the drip line, the separation energy of the last nucleon(s) becomes small. The valence nucleons of such loosely bound nuclei may have a very extended density distribution, called "halo". The necessary conditions for the halo formation have been intensively discussed. It was concluded that the nuclear states with small binding energy and low angular momentum may form halos. The halo structure manifests itself in the different types of reaction, in particular, in the large interaction cross section and in the narrow momentum distribution of the reaction products in the processes of nuclear breakup and Coulomb dissociation. The experimental methods applied for studying halo nuclei were mainly measurements of the total interaction cross sections and investigations of halo breakup reactions. These methods were widely used in nuclear structure research at GSI, where clean and intense secondary beams of exotic nuclei have been obtained with the aid of FRS.

The IKAR Collaboration at GSI proposed a new approach to study the spatial structure of exotic nuclei by small-angle proton elastic scattering at intermediate energy in inverse kinematics (Experiment S105). An advantage of proton scattering experiments at intermediate energy (about 700 MeV/u) as compared to similar experiments at low energy is that at intermediate energy there exists a rather accurate multiple scattering theory of Glauber, which can relate the measured cross sections with the studied density distributions in quite an unambiguous way. The scattering of protons from the nuclear halo is confined to small scattering angles. Therefore, in order to study the spatial structure of halo nuclei it is important to measure with high accuracy the differential cross sections for proton scattering at small momentum transfers.

The recoil detector IKAR, developed and built at PNPI [1], was used as active hydrogen target in a combination with a spectrometer for measurements of projectile scattering angles. The entire experimental setup is shown in Fig. 1. The ALADIN magnet and a scintillator wall behind it was used for safe separation of the projectile break-up channels. In Experiment S105, the absolute differential cross sections $d\sigma/dt$ for p^{4}He, p^{6}He, p^{8}He (in 1993) and p^{6}Li, p^{8}Li, p^{9}Li, p^{11}Li (in 1996) were measured in the range $0.002 \geq |t| \geq 0.050$ (GeV/c)^2 of the four-momentum transfer squared t.

For establishing the nuclear density distributions from the measured cross sections, the Glauber multiple scattering theory was applied (Fig. 2). It was shown that a positive curvature in $\log(d\sigma/dt)$ at

small momentum transfers can be used as a qualitative indication of possible halo existence (Fig. 3). An important feature of the method is that it permits to obtain from the data simultaneously the matter, core and valence nucleon(s) r.m.s. radii. Results of the S105 experiment are presented in Table 1. The ratio of the valence nucleon to core nucleon radii gives a parameter for a quantitative measure of the halo structure [2]. The obtained results clearly demonstrate the halo structure of ^{6}He, ^{8}He and ^{11}Li, the most prominent halo being observed for ^{11}Li (Fig. 4). In the case of ^{6}Li, which is the N=Z nucleus, the matter density distribution determined from the data on small-angle proton scattering is in good agreement with the proton distribution deduced from the known data on electron scattering [3]. The results of this experiment have been published [3-7].

New measurements (Experiment S247) with the same experimental techniques were performed on B and Be ion beams at GSI in 2005 and 2006. Small-angle proton elastic scattering from the ^{7}Be, ^{9}Be, ^{10}Be, ^{11}Be, ^{12}Be, ^{14}Be and ^{8}B nuclei was studied. The most interesting among these nuclei are ^{8}B, in which the proton halo may exist, and ^{11}Be, ^{14}Be, for which significant neutron halos are expected. An analysis of the experimental data is in progress. Some preliminary results obtained for Be isotopes are demonstrated in Fig. 5.

Here we propose to study the nuclear spatial structure of neutron-rich boron and carbon isotopes with the same method which was used in Experiments S105 and S247. This method is unique and is available at present only at GSI.

The heaviest isotopes in the B and C chains which can be obtained at GSI with sufficient intensity (more that 10^3 particles/s) are ^{15}B and ^{17}C. A systematic study of one-neutron removal reactions for a range of neutron-rich *psd*-shell nuclei in boron and carbon chains has been carried out in Ref. [8]. The measured longitudinal momentum distributions of the core fragments are shown in Fig. 6. The crossing of the N=8 shell closure, when going from light to heavier B and C isotopes, may be associated with a marked reduction in the width of the core momentum distributions for ^{14}B, ^{15}B and ^{15}C. In the same experiment [8], it was shown that ^{14}B and ^{15}C exhibit enhanced one-neutron removal cross sections with respect to the neighboring isotopes. Given these facts, it has been suggested that ^{14}B with a low neutron separation energy (S_n=0.97 MeV) has a halo like structure.

We propose to study the isotopic chain ^{11}B, ^{13}B, ^{14}B and ^{15}B by small-angle proton elastic scattering (as was made for He and Li isotopes), which will allow to explore the evolution of nuclear size and structure with increasing the isospin. The r.m.s. matter radii of B (and C) isotopes were deduced from the total interaction cross-section measurements at high energy [9] and were extracted from the reaction cross sections at lower energy [10] (Fig. 7). Disagreement of these results is obvious. Our measurements should clear up the situation.

Information on halo structures in carbon isotopes is rather contradictory. Some carbon nuclei (^{15}C,^{17}C,^{19}C) have relatively small separation energies, so a halo structure in these nuclei are expected. Experimental studies gave evidence of one neutron halo structure in ^{19}C and ^{15}C [11,12]. As for ^{17}C, the broad parallel momentum distribution of fragments ^{16}C has shown no halo structure in ^{17}C [13]. On the other hand, the existence of a tail in the density distribution was suggested [14] in a study of the density distribution of ^{17}C from the reaction cross section measurements at low energy. Contradictory results were also obtained for ^{16}C. In spite of a relatively large neutron separation energy, 2n-halo structure in ^{16}C was suggested [15] in order to explain a large enhancement in the reaction cross-section. On the other hand, a relatively broad momentum distribution of breakup fragments for ^{16}C [8,16] shows no halo formation in this nucleus.

For a systematic investigation of the carbon chain, we intend to study ^{14}C, ^{15}C, ^{16}C, and ^{17}C. Here ^{14}C is assumed to be the core nucleus for ^{15}C. We hope to see the halo and skin development with increasing the number of neutrons. In addition, it is interesting to measure also the reference N=Z nucleus ^{12}C, for which the charge radius is measured with high precision.

The sensitivity of the differential cross section to the radial shape of the nuclear matter distribution in the case of the proposed experiment for ^{14}B and ^{17}C one-neutron halo nuclei is illustrated in Fig. 8 by simulation calculations. In both figures, two different density distributions are presented (upper plot). The non-halo structures are described by a Gaussian (G), while the halo structures are assumed

to be the sum of two Gaussians (GG) – one for the core nucleons and the other for the halo nucleon. R_c and R_h in Fig. 8 denote the r.m.s. radii of the core and halo nucleon distributions, respectively. Both density distributions have the same nuclear matter radius R_m, but essentially different radial shape. The lower plots show in logarithmic scale the calculated cross sections related to these densities. To see more clearly the sensitivity of the cross sections curvature to the density shape, the calculated cross sections are divided by exponential functions. The values R_m=2.50 fm and R_h=5.0 fm were chosen for ^{14}B; R_m=2.50 fm and R_h=4.45 fm were adopted for ^{15}C. It is seen that the t-dependence of the cross sections for the two cases considered (^{14}B and ^{15}C nuclei with a halo and without a halo) are significantly different, which allows one to obtain information on the halo structure of the studied nuclei by measuring $d\sigma/dt$ at small momentum transfers.

Table 2 presents the beam time demand for the investigation of the nuclear structure of neutron-rich boron and carbon isotopes in the proposed experiment.

References

[1] A.A. Vorobyov et al., Nucl. Instr. Meth. 119 (1974) 509.
[2] L.V. Grigorenko et al., Phys. Rev. C57 (1998) R2099.
[3] A.V. Dobrovolsky et al., Nucl. Phys. A766 (2006) 1.
[4] G.D. Alkhazov et al. Phys. Rev. Lett. 78 (1997) 2313.
[5] S.R.Neumaier et al., Nucl. Phys. A712 (2002) 247.
[6] G.D.Alkhazov et al., Nucl. Phys. A712 (2002) 269.
[7] P. Egelhof et al. Eur. Phys. J. A15 (2002) 27.
[8] E. Sauvan et al. Phys. Rev. C69 (2004) 044603.
[9] A. Ozawa et al., Nucl. Phys. A693 (2001) 32.
[10] E. Liatard et al. Europhys.Lett. 13(1990)401.
[11] A. Ozawa et al., Nucl. Phys. A691 (2001) 599.
[12] B. Jonson, Phys. Rep. 389 (2004) 1.
[13] T. Baumann et al., Phys. Lett. B439 (1998) 256.
[14] C. Wu et al., Nucl. Phys. A739 (2004) 3.
[15] T. Zheng et al., Nucl. Phys. A709 (2002) 103.
[16] T. Yamaguchi et al., Nucl. Phys. A734 (2004) E73.

Table 1.
Summary of the results obtained for helium and lithium isotopes in Experiments S105. The values R_m, R_c and R_v denote the r.m.s. radii of the matter, core and valence nucleon(s) distributions, κ is the ratio R_v/R_c.

Nucleus	R_m, fm	R_c, fm	R_v, fm	$\kappa = R_v/R_c$
^{4}He	1.49(3)	–	–	–
^{6}He	2.45(10)	1.88(12)	3.31(28)	1.76
^{8}He	2.53(8)	1.55(15)	3.22(14)	2.08
^{6}Li	2.44(7)	2.11(17)	3.00(34)	1.42
^{8}Li	2.50(6)	2.48(7)	2.58(48)	1.03
^{9}Li	2.44(6)	2.20(6)	3.12(28)	1.41
^{11}Li	3.71(20)	2.53(3)	6.85(58)	2.71

Table 2.
Beam time demand for investigation of nucleon density distributions of B and C isotopes.

	Primary beam	Isotope	Secondary beam intensity (sec^{-1})	Number of shifts
B isotopes	^{18}O	^{11}B	$5\cdot10^3$	7
	^{18}O	^{13}B	$5\cdot10^3$	7
	^{18}O	^{14}B	$5\cdot10^3$	7
	^{18}O	^{15}B	$5\cdot10^3$	7
	Adjustment of apparatus and beam development			4
C isotopes	^{18}O	^{12}C	$5\cdot10^3$	7
	^{18}O	^{14}C	$5\cdot10^3$	7
	^{18}O	^{15}C	$5\cdot10^3$	7
	^{18}O	^{16}C	$5\cdot10^3$	7
	^{22}Ne	^{17}C	$5\cdot10^3$	7
	Adjustment of apparatus and beam development			4
Total number of shifts				71

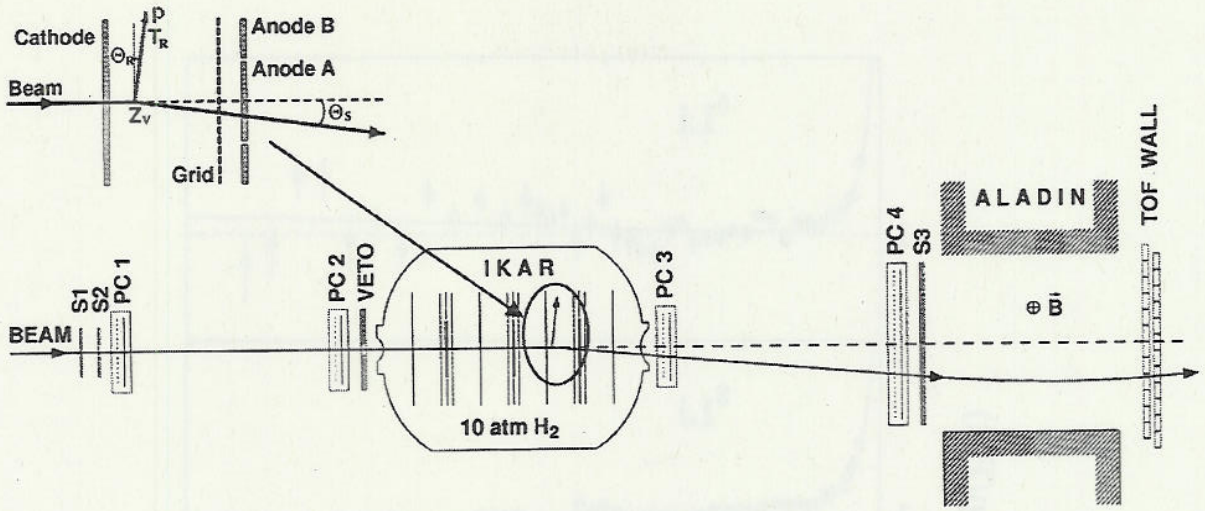

Fig. 1. Schematic view of the experimental set-up for small-angle proton elastic scattering on exotic nuclei in inverse kinematics. The central part shows the hydrogen-filled ionization chamber IKAR, which serves simultaneously as target and detector system for recoil protons. In six independent sections of this detector the recoil energy T_R, the recoil angle Θ_R and the vertex point Z_v are determined (see insert). The forward spectrometer consisting of four multi-wire proportional chambers PC1-PC4 determines the scattering angle Θ_S of the projectile. The scintillation counters S1-S3 and VETO are used for beam identification and triggering. The ALADIN magnet with a position sensitive scintillator wall behind allows to identify the scattered beam particle and discriminate breakup channels.

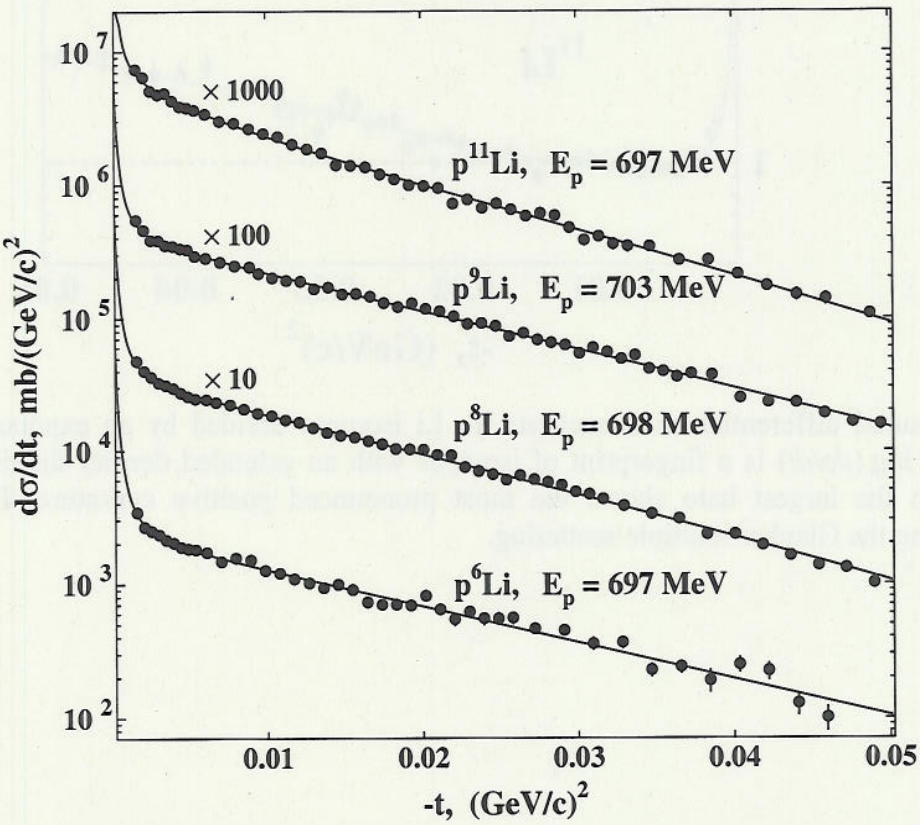

Fig. 2. Absolute differential cross sections $d\sigma/dt$ versus the four momentum transfer squared t for Li isotopes (Experiment S105). Plotted lines are obtained by calculations using the Glauber multiple scattering theory.

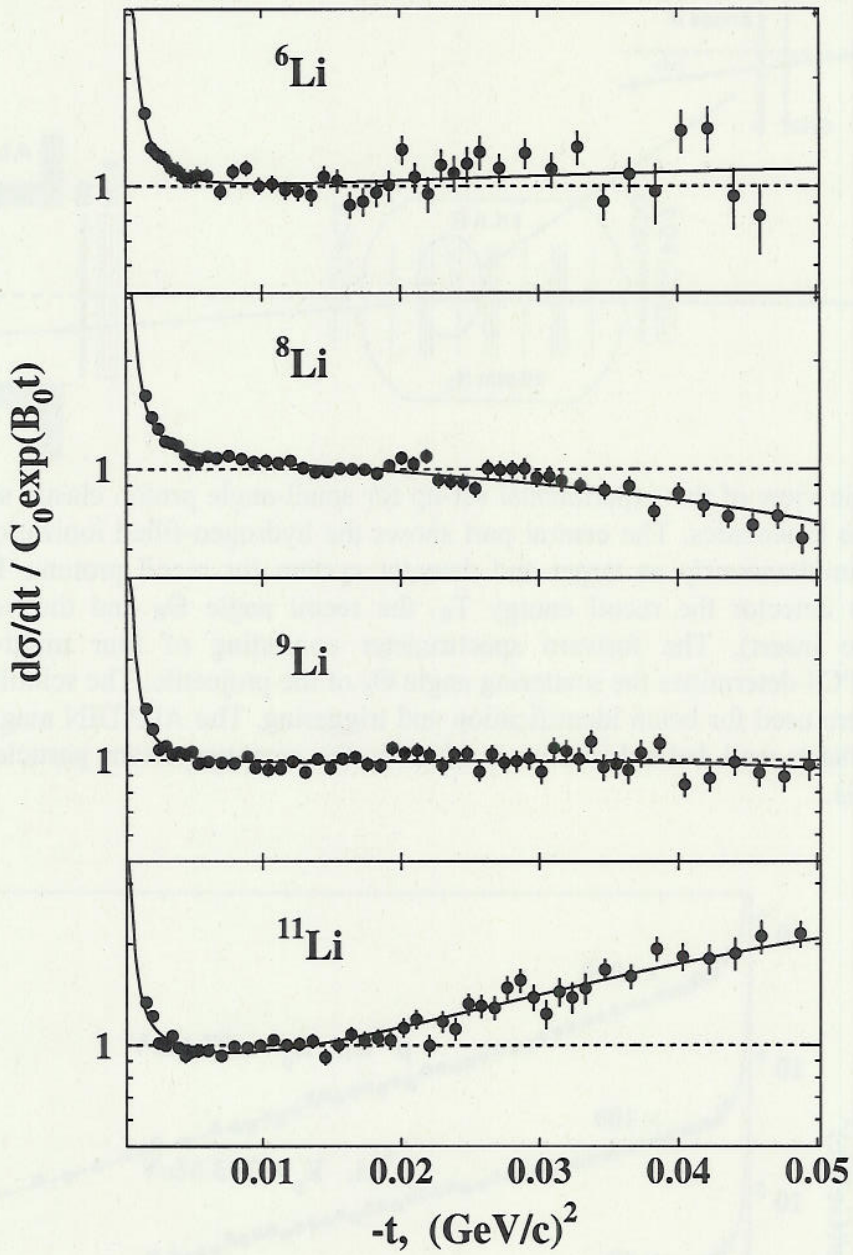

Fig. 3. Measured differential cross sections for Li isotopes divided by an exponent. The positive curvature in log ($d\sigma/dt$) is a fingerprint of isotopes with an extended density distribution. The ^{11}Li nucleus with the largest halo shows the most pronounced positive curvature. Plotted lines are obtained using the Glauber multiple scattering.

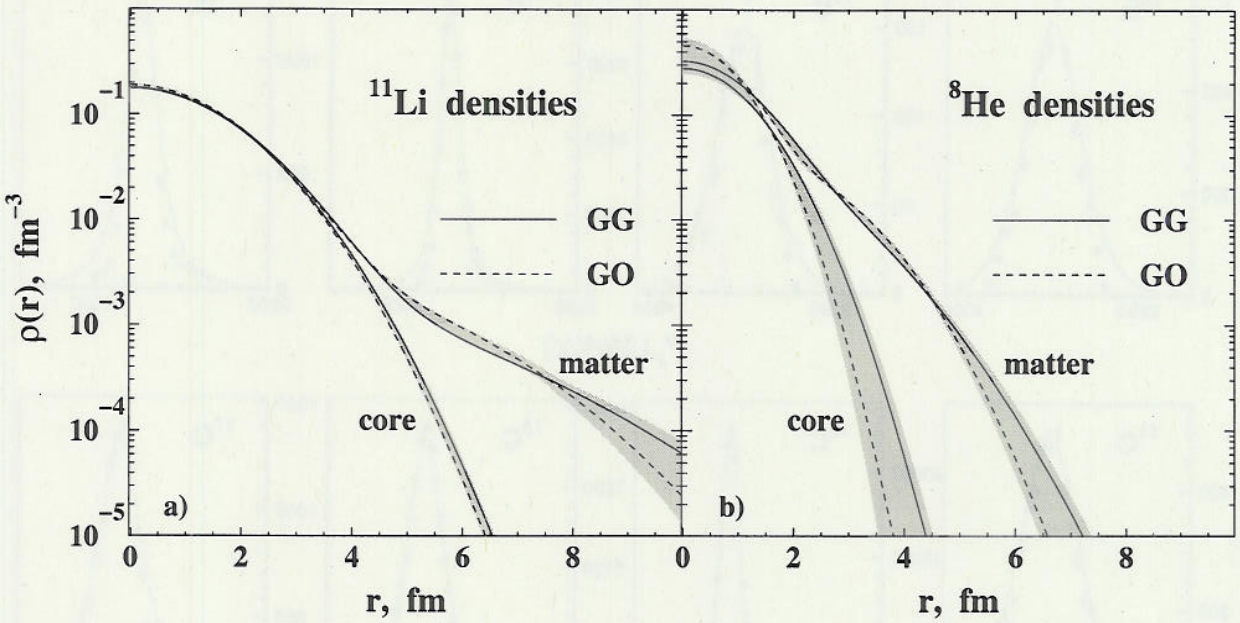

Fig. 4. Nuclear core and total matter density distributions $\rho(r)$ in ^{11}Li (left side) and ^{8}He (right side) deduced from the experimental data. Labels denote different parameterizations of phenomenological density distributions used in the analyses (for details see Ref. [3]). The shaded areas represent the envelopes of the matter and core density variations within the model parameterizations applied, superimposed by the statistical errors.

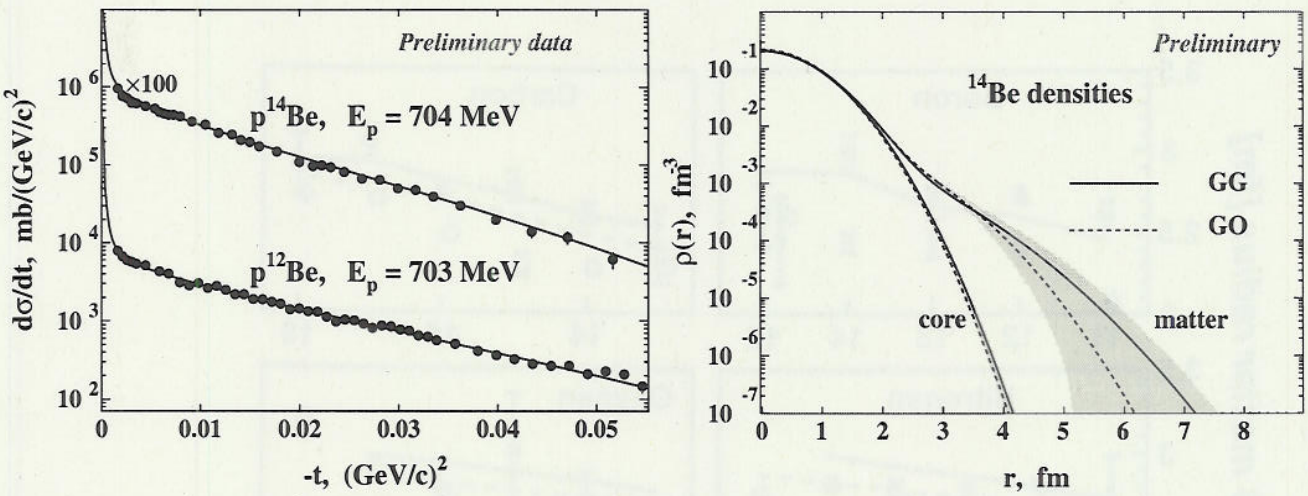

Fig. 5. Absolute differential cross sections $d\sigma/dt$ for Be isotopes (left side). Parameters of nuclear core and total matter density distributions $\rho(r)$ in ^{14}Be (right side) deduced from experimental data are: R_m = 3.15 (12) fm, R_c = 2.66 (3) fm, R_h = 5.19 (52) fm for GG; R_m = 3.11 (9) fm, R_c = 2.61 (3) fm, R_h = 5.18 (36) fm for GO (preliminary results). The halo structure of ^{14}Be is evident.

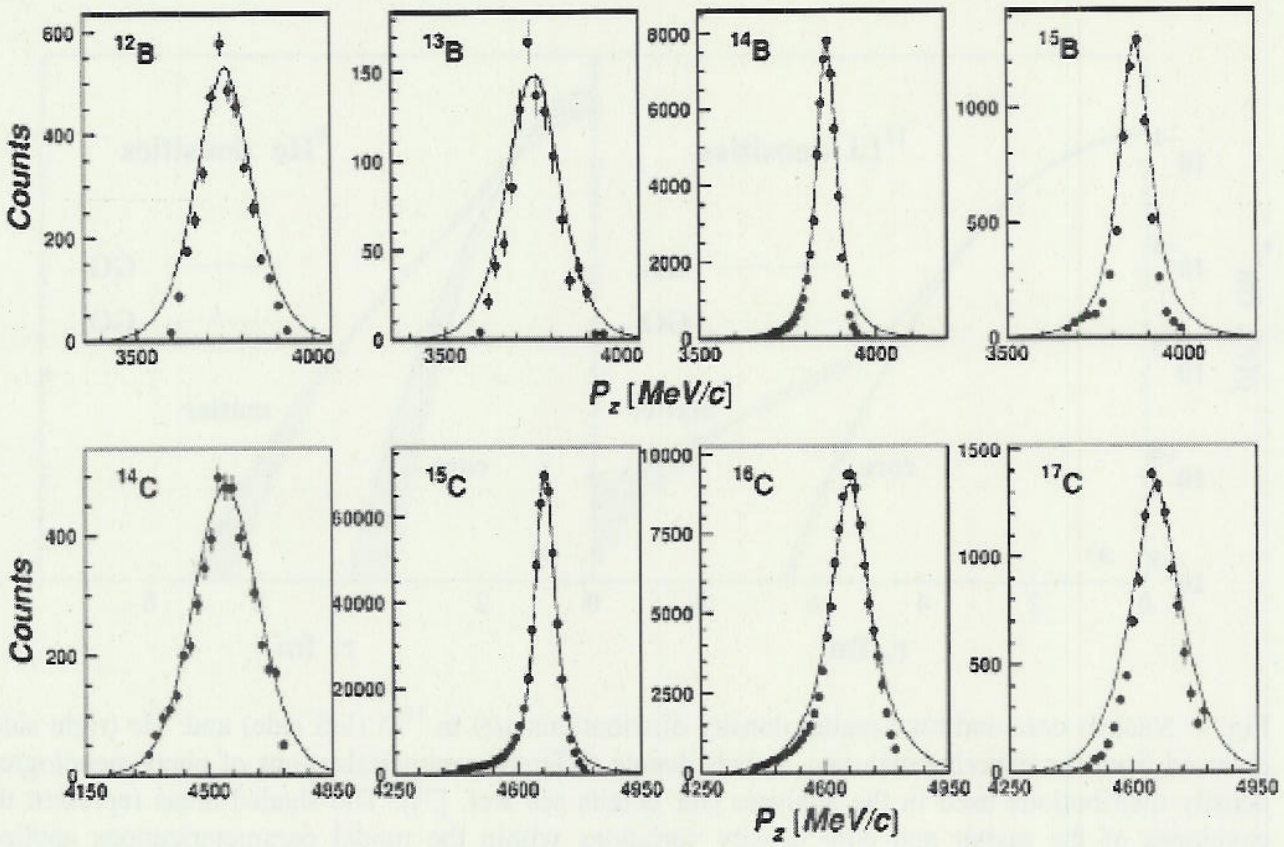

Fig. 6. Core fragment longitudinal momentum distributions for boron and carbon isotopes obtained with a carbon target [8]. Solid line – Glauber model calculations.

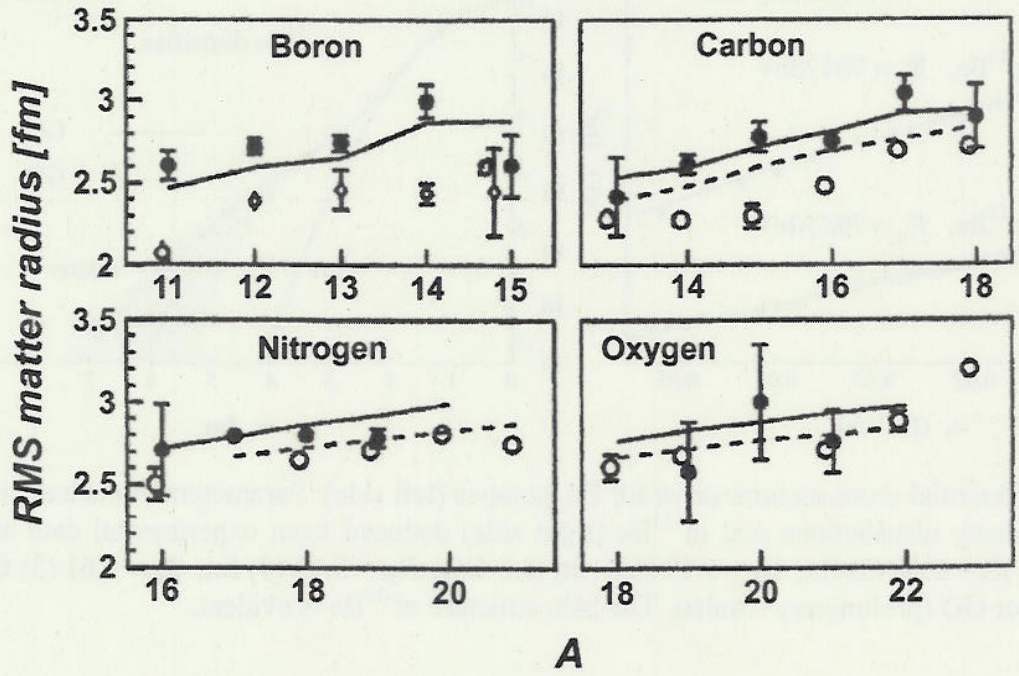

Fig. 7. Experimental values for r.m.s. matter radii obtained at relativistic energies [9] (open circles and diamonds) and at low energies [10] (filled circles). Solid lines – Hartree-Fock calculations, dashed lines – relativistic mean field calculations. (From [8]).

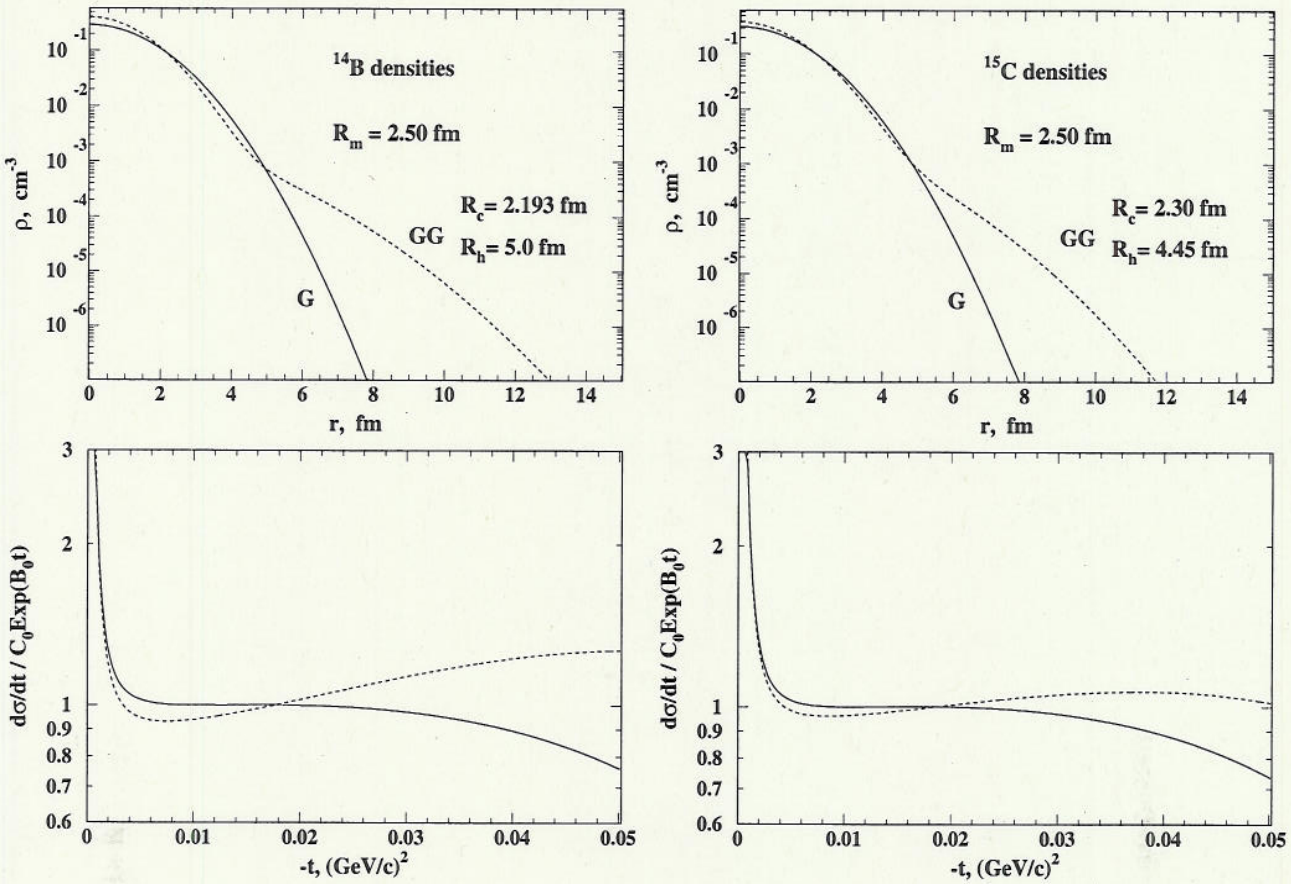

Fig. 8. Sensitivity of the differential elastic proton scattering cross section divided by an exponent on the halo structure in ^{14}B.and ^{15}C. The cross sections (lower plot) are calculated for the assumption of a one Gaussian (G) and a two Gaussian (GG) density distribution (upper plot), both having the same total matter radius R_m= 2.50 fm .